

Structure–Property Relationships in Phosphole-Containing π -Conjugated Systems: A Quantum Chemical Study

David Delaere, Minh Tho Nguyen,* and Luc G. Vanquickenborne

Department of Chemistry, University of Leuven, Celestijnenlaan 200F, B-3001 Leuven, Belgium

Received: June 3, 2002; In Final Form: September 13, 2002

The aim of this theoretical study is to provide an in-depth interpretation of the UV–vis absorption spectra and electrochemical data of two series of 2,5-dipyridyl- and 2,5-dithienylphosphole derivatives containing σ^3 - or σ^4 -P atoms. The geometric and electronic structures of those phosphole-containing π -conjugated systems were investigated using density functional theory (DFT). To assign the absorption peaks observed in the UV–vis absorption spectra, we computed the energies of lower-lying excited states within the adiabatic approximation of time-dependent DFT (TDDFT). All DFT calculations were performed using the B3LYP functional and the split valence plus polarization SV(P) basis set. To elucidate structure–property relationships, we studied in a systematic way the influence of different structural modifications on the electronic structure and emphasized the corresponding consequences for the electrochemical and optical properties. More specifically, we considered successively the influence of pyridyl and thienyl substituents at the α -position, flattening of the P atom, oxidation of the P atom by elemental sulfur, and fusion of a saturated six-membered ring onto the phosphole core.

Introduction

π -Conjugated organic oligomers and polymers are showing increasing potential as active components for a wide range of semiconducting devices,¹ including field effect transistors,² light-emitting diodes³ (LEDs), and photovoltaic components.⁴ The electrical and optical behavior of these materials originate from their typical geometric and electronic structure; hence, their electronic and optical properties could in principle be fine-tuned by manipulation of their chemical structure. For example, the width of the energy gap, which determines the optical properties of LEDs, can be changed upon chemical substitution. Because quantum mechanical methods are able to reliably describe such structure–property relationships, they are of great help when designing materials with enhanced (opto)electronic properties.⁵

Five-membered heterocycles such as pyrrole and thiophene have widely been used as building blocks for the design of well-defined linear π -conjugated oligomers and polymers. Also, phosphole (Ph), the P analogue that possesses a unique geometric and electronic structure, has recently attracted more attention^{6–8} as a promising building block for the engineering of π -conjugated systems with a chemically tunable energy gap. In contrast to pyrrole and thiophene, Ph⁹ is a nonplanar and nonaromatic five-membered ring since it contains a rigid pyramidal tricoordinated phosphorus atom (σ^3 -P atom), which prevents strong cyclic π -conjugation between the phosphorus lone pair and the *cis*-1,3-butadiene unit. In oligomers or polymers, the Ph P atom however retains a versatile reactivity, which thus offers an interesting possibility of tuning their (opto)-electronic properties by chemical modification.

In this context, Réau and co-workers^{6–8} prepared and evaluated the photophysical and electrochemical properties of two series of 2,5-dipyridylphosphole (PyrPhPyr) and 2,5-dithienylphosphole (ThPhTh) derivatives containing σ^3 - or σ^4 -P

atoms. These authors made several structural variations for tuning the Ph's electronic properties and elucidating the structure–property relationships. For example, heteroaryl substituents such as pyridyl and thienyl were introduced at the α -position (the 2,5-positions) of the Ph ring in conjunction with a variation of the size of the fused carbocycle and the substituents on phosphorus. Finally, chemical modification of the nucleophilic P atom was performed. Crystal structures, UV–vis absorption and fluorescence spectra, and electrochemical data of those compounds were abundantly reported. Nyulászi⁸ performed *ab initio* calculations on the parent molecules and discussed the energetics of different possible conformers of 2,5-diheteroarylphospholes as well as the geometric and electronic structure of 2,5-dithienylheterocyclopentadienes and derivatives. Analysis of the electronic structure data was however restricted to the highest occupied molecular orbital (HOMO) and lowest unoccupied molecular orbital (LUMO) energies. Some structure–property relationships of these model compounds were suggested on the basis of the above-mentioned experimental and theoretical data. The ThPhTh derivatives appeared to be particularly interesting, as their optical and electrochemical properties vary over a wide range depending on the nature of the phosphorus moiety. These properties prompted them to prepare corresponding polymers by electrooxidation. Nevertheless, several questions related to structure–property relationships were not answered yet. For example, we did not find in previous papers^{6–8} an explanation for the opposite effect in the absorption spectra within the pyridyl and thienyl series when oxidizing the P atom by elemental sulfur.

The aim of the present work is to provide an in-depth interpretation of the UV–vis absorption spectra and electrochemical data of the two series of PyrPhPyr and ThPhTh derivatives obtained by Réau and co-workers.^{6–8} To assign the absorption peaks, we computed the vertical lower-lying excited states. Furthermore, the redox potentials were related to the inherent electronic structure rather than ascribed to the electron-

* To whom correspondence should be addressed. Fax: 32-16-32 79 92. E-mail: minh.nguyen@chem.kuleuven.ac.be.

rich or electron-poor character of the substituents. The following strategy was used to elucidate structure–property relationships: we studied in a systematic manner the influence of different structural modifications on the electronic structure, and from there, we derived the consequences for the electrochemical and optical properties. We paid particular attention to the influence of pyridyl and thienyl substituents at the α -position, flattening of the P atom, oxidation of the P atom using elemental sulfur, and fusion of a saturated six-membered ring onto the Ph core.

Computational Details

Geometric and electronic structures of the considered Ph-containing π -conjugated systems were investigated making use of density functional theory (DFT).¹⁰ Lower-lying excited states were computed within the framework of the adiabatic approximation of time-dependent DFT (TDDFT).¹¹ All DFT calculations were performed using the B3LYP functional and the split valence plus polarization SV(P)¹² basis set.

As shown in our previous study on Ph monomers,¹³ a combination of both geometric (Jug index, JI) and magnetic (nucleus-independent chemical shift, NICS) criteria leads to an interesting approach to analyze the π -electron delocalization in conjugated heterocyclic systems. Because we are considering α -substituted heteroarylphosphole derivatives, the interring bond distances ($d_{C\alpha}$) are also taken into account in order to reflect the strength of π -electron conjugation between the Ph core and the heteroaryl substituents.

The JI¹⁴ is defined in terms of the deviations of the individual C–C bond lengths (r_i) from the mean carbon–carbon bond length (r) and constitutes a measure of the bond length alternation (π -electron conjugation) in the *cis*-1,3-butadiene unit. Accordingly, the π -conjugation along the *cis*-1,3-butadiene unit will be more pronounced if the JI becomes closer to one. The JI is influenced by both the aromaticity of the Ph core and the linear π -conjugation toward the heteroaryl substituents.

In the NICS approach,¹⁵ the absolute magnetic shieldings are computed at the ring center (nonweighted mean of the heavy atom coordinates). With respect to the familiar NMR chemical shift convention, the sign of the computed values is reversed: negative NICS values denote aromaticity; the more negative the NICS value is, the more aromatic the system is. As a reference point, we would like to mention the NICS value for benzene, which amounts to -10.5 ppm. The NICS values were computed making use of the GIAO-HF/6-311G* method.¹⁶ The Turbomole program¹² was employed for optimizing molecular geometries and calculating lower-lying excited states, whereas the Gaussian 98 program¹⁶ was used in computing NICS values.

Results and Discussion

Influence of Heteroaryl Substituents. Geometric Structure. Solid state structure analysis revealed the pyridyl rings of PyrPhPyr⁶ derivatives to have a syn arrangement with respect to the central Ph ring. In contrast, the lowest energy conformation of ThPhTh⁷ derivatives was found to be the anti arrangement. The simplicity of the ¹³C NMR spectra of those 2,5-diheteroarylphospholes favors symmetrical structures. However, the theoretical calculations performed by Nyulási⁸ have shown that the energy differences between possible conformers are small and barriers to rotation are rather low (12–16 kJ/mol) in those compounds.

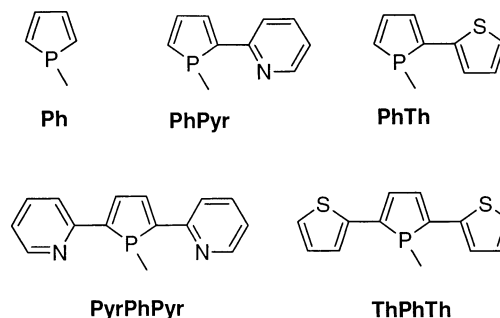


Figure 1. Molecules considered include Ph, PhPyr, PhTh, PyrPhPyr, and ThPhTh.

TABLE 1: Influence of α -Substitution on the Geometry of the Ph Core

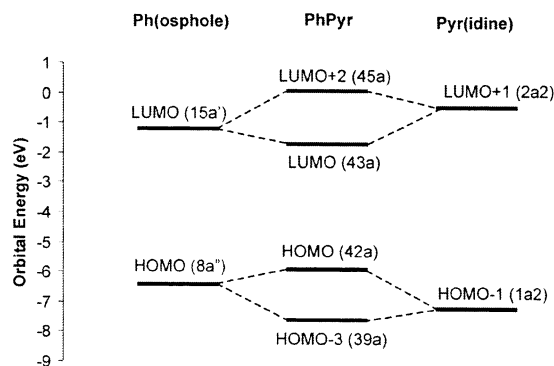
	Ph	PhPyr	PyrPhPyr	PhTh	ThPhTh
sym	C_s	C_1	C_s	C_1	C_s
Ph core					
P–C ^a	1.818	1.817/1.829 ^b	1.827	1.816/1.842	1.841
C=C	1.360	1.363/1.370 ^b	1.373	1.361/1.371	1.373
C–C	1.461	1.452	1.443	1.452	1.442
Σ CPX ^c	292.7	293.4	294.1	290.6	288.5
JI	0.74	0.81	0.87	0.81	0.88
NICS ^d	-5.5	-4.2	-3.0	-4.3	-2.8
Interring					
α^e		3.7	5.1	16.7	14.4
$d_{C\alpha}^a$		1.465	1.464	1.450	1.447

^a Bond lengths are given in Ångströms. ^b Largest value corresponds with the substituted side. ^c Bond and dihedral angles are given in degrees. ^d NICS values are given in ppm.

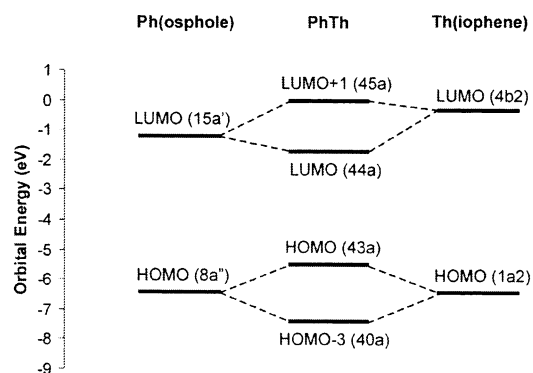
We have optimized the geometry of the syn 2-pyridylphospholes (PhPyr) and the anti 2-thienylphospholes (PhTh) with no symmetry (C_1), whereas the syn 2,5-dipyridylphospholes (PyrPhPyr) and the anti 2,5-dithienylphospholes (ThPhTh) were optimized within C_s symmetry. Above-mentioned structures are presented in Figure 1. Table 1 records the influence of α -substitution on the geometry of the Ph core.

The pyridyl and Ph rings are computed to be nearly coplanar, whereas a small deviation from coplanarity (around 15°) is found between thienyl and Ph. Heteroaryl substitution at the α -position of Ph is found to lengthen the P–C bond and to increase the π -conjugation over the *cis*-1,3-butadiene unit, as reflected in an increase of the JI. The aromaticity of the Ph ring weakens as shown by a less negative NICS value. This indicates that the π -conjugation toward the phosphorus atom (cyclic π -conjugation) weakens as a result of π -conjugation toward the heteroaryl substituents (linear π -conjugation). Both JI and NICS values also show that the π -conjugation over the *cis*-1,3-butadiene unit becomes more pronounced for disubstituted phospholes (PyrPhPyr, ThPhTh) as compared to the monosubstituted ones (PhPyr, PhTh), which is as expected, taking into account the more extended linear π -conjugation. As a matter of fact, the interring bond distance ($d_{C\alpha}$) between thienyl and Ph is smaller than that between pyridyl and Ph. Moreover, the lengthening of the P–C bond and the pyramidalicity of the P atom, as reflected by the Σ CPX value, is more pronounced in thienyl derivatives. Therefore, we concur with the conclusion of Nyulási⁸ that the most effective linear π -conjugation is achieved in thienyl-substituted phospholes (PhTh, ThPhTh).

Electronic Structure. The valence π -MOs of PhX and XPhX with X = Pyr(idine) or Th(iophene) are formed by overlapping the π -MOs of Ph and X to overlap. The UV–vis absorption spectrum basically results from $\pi^* \leftarrow \pi$ transitions. The wave-



(a)



(b)

Figure 2. Orbital interaction diagrams describing the formation of the frontier MOs of (a) PhPyr and (b) PhTh.

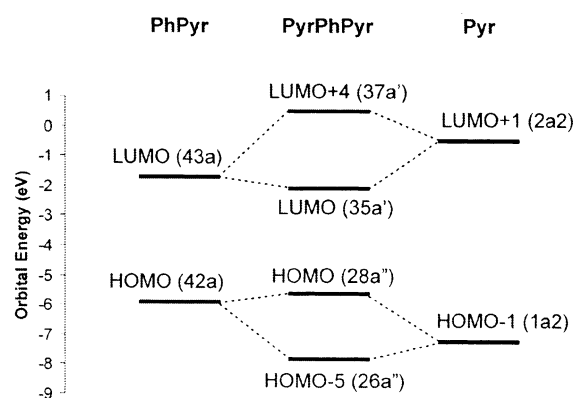
length of absorption (λ_{\max}) then forms a measure of the separation of the energy levels of the orbitals concerned. The electronic excitation energy is related to the wavelength of absorption by

$$E \text{ (kJ/mol)} = \frac{1.19 \times 10^5}{\lambda \text{ (nm)}}$$

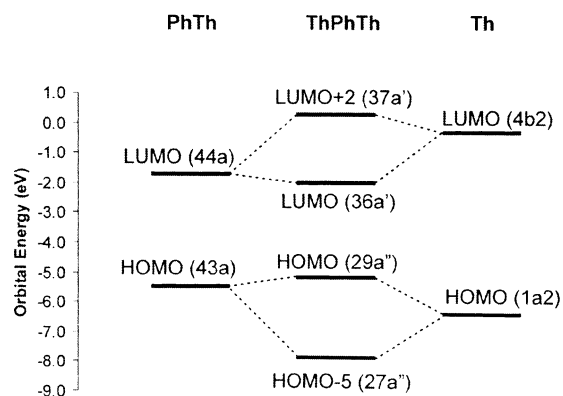
The energy gap between both frontier orbitals, the HOMO, and the LUMO gives a rough estimate for the lowest electronic excitation energy.

Orbital interaction diagrams that describe the formation of the frontier MOs of PhX and XPhX are shown in Figures 2 and 3, respectively. The shape of the considered π and π^* MOs is presented in Figures 4 and 5, respectively. The frontier orbital energies and a description of the lowest allowed singlet $\pi^* \leftarrow \pi$ transition are given in Table 2.

Figure 2 together with Figures 4 and 5 show that the HOMO of PhPyr or PhTh represents an antibonding interaction between, on one hand, the HOMO (8a'') of Ph and, on the other hand, the HOMO-1 (1a₂) of Pyr or the HOMO (1a₂) of Th, respectively. On the contrary, the LUMO of PhPyr or PhTh corresponds with a bonding interaction between the LUMO (15a') of Ph and the LUMO+1 (2a₂) of Pyr or the LUMO (4b₂) of Th, respectively. When the molecular orbitals of Ph and Pyr or Ph and Th are brought into conjugation, the energy level of the HOMO is raised and that of the LUMO is lowered. Figure 3 shows that extension of the π -conjugated system by substituting a second heteroaryl ring at Ph further lowers the HOMO–LUMO gap.



(a)



(b)

Figure 3. Orbital interaction diagrams describing the formation of the frontier MOs of (a) PyrPhPyr and (b) ThPhTh.

The HOMO-1 orbital energy of Pyr is at -7.2 eV and lies 0.8 eV lower in energy than the HOMO of Ph, which is at -6.4 eV. The HOMOs of Ph and Th have very nearly the same energy. Because MOs interact less strongly as their energies diverge, the HOMO energy of PhPyr is less raised and lies 0.3 eV lower than the HOMO energy of PhTh. The LUMO+1 orbital of Pyr and the LUMO orbital of Th have similar energies. They are 0.7 and 0.9 eV, respectively, higher in energy than the LUMO of Ph, which is at -1.2 eV. As a consequence, the LUMO energies of PhPyr and PhTh are virtually identical at -1.7 eV. The HOMO energy of PyrPhPyr and ThPhTh is at -5.6 and -5.2 eV, respectively, and their LUMO energy is at -2.1 and -2.0 eV, respectively.

If we take the above results into account, we could expect that PyrPhPyr would have a higher oxidation potential than ThPhTh and that both derivatives have a similar reduction potential. First, anodic (E_{pa}) peak potentials⁸ of 2,5-diheteroarylphospholes confirm that PyrPhPyr is in fact less easily oxidized than ThPhTh. Because the cathodic (E_{pc}) peak potential of ThPhTh could not unambiguously be assigned, no statement is given about the reduction potential.

Table 2 shows that the singlet 1A'' state of Ph and heteroarylphospholes involves the LUMO–HOMO excitation and therefore corresponds to the lowest allowed $\pi^* \leftarrow \pi$ transition. At first, when comparing the calculated absorption wavelength (λ_{\max}) of PhX with that of XPhX, we see that the more extended the π -conjugated system, the longer λ_{\max} or the lower the corresponding excitation energy. An explanation for this

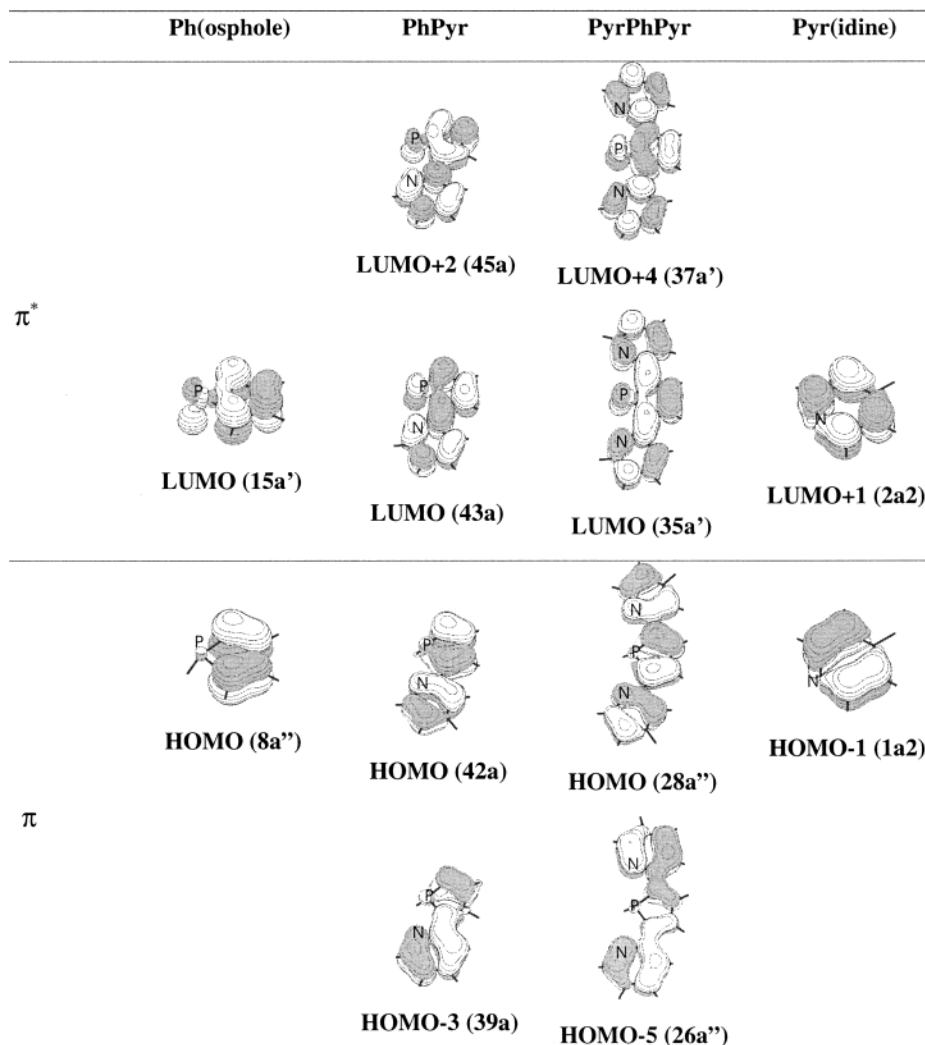


Figure 4. Shape of the π and π^* MOs involved in the orbital interaction diagrams that describe the formation of the frontier MOs of PhPyr and PyrPhPyr.

TABLE 2: Frontier Orbital Energies and a Description of the Lowest Allowed Singlet $\pi^* \leftarrow \pi$ Transitions of Ph, PhPyr, PyrPhPyr, PhTh, and ThPhTh

		Ph	PhPyr	PyrPhPyr	PhTh	ThPhTh
$1^1A''$	ϵ_{LUMO}^a	-1.2 (15a')	-1.7 (43a)	-2.1 (35a')	-1.7 (44a)	-2.0 (36a')
	ϵ_{HOMO}	-6.4 (8a'')	-5.9 (42a)	-5.6 (28a'')	-5.6 (43a)	-5.2 (29a'')
	λ_{max}^b	262	326	383	347	422
		15a' \leftarrow 8a''	43a' \leftarrow 42a	35a' \leftarrow 28a''	44a' \leftarrow 43a	36a' \leftarrow 29a''
	f^c	0.05	0.29	0.71	0.32	0.66

^a Frontier orbital energies are given in electronvolts. ^b The computed λ_{max} values are given in nanometers. ^c Oscillator strengths (f).

observed red shift is given by the aforementioned decrease of the HOMO–LUMO gap when extending the π -conjugated system by substitution of a second heteroaryl ring at Ph. A second finding is that the red shift induced by pyridyl is smaller than the one induced by thienyl, since the HOMO of (Pyr)-PhPyr is less destabilized than the one of (Th)PhTh and both LUMOs are at virtually the same energy. Furthermore, when comparing the oscillator strength (f) of PhX with that of XPhX, we see that the longer the π -conjugated system is, the larger f or the more intense the absorption becomes.

Influence of Flattening the P Atom. Geometric Structure. In its equilibrium structure, Ph is nonaromatic since it contains a pyramidal tricoordinated phosphorus atom, which prevents a strong cyclic π -conjugation between the phosphorus lone pair and the *cis*-1,3-butadiene unit. On the contrary, planar Ph is aromatic. Thus, regulation of the pyramidalicity of the phosphorus

atom offers an interesting possibility to control the aromaticity (cyclic π -conjugation) in the Ph core. Indeed, the pyramidalicity can be controlled by substituents. For example, bulky substituents at the P atom tend to reduce the pyramidalicity.¹⁷ Some alkylarylphospholes¹⁸ even become aromatic although they are not completely planar. On the other hand, earlier computational investigations^{13,18} have shown that a phenyl substituent at phosphorus causes practically no change in bond lengths, even though the sum of CPX angles (ΣCPX) differs from that of the parent. Thus, substituting a phenyl group at phosphorus does not alter the Ph aromaticity. Another possibility to flatten the P atom is the use of π -acceptor groups either at phosphorus or at the neighboring α -carbons.^{13,19}

A representation of 2,5-diheteroarylphospholes with a constrained planar P atom is given in Figure 6. Table 3 records the influence of flattening the P atom on geometric structures.

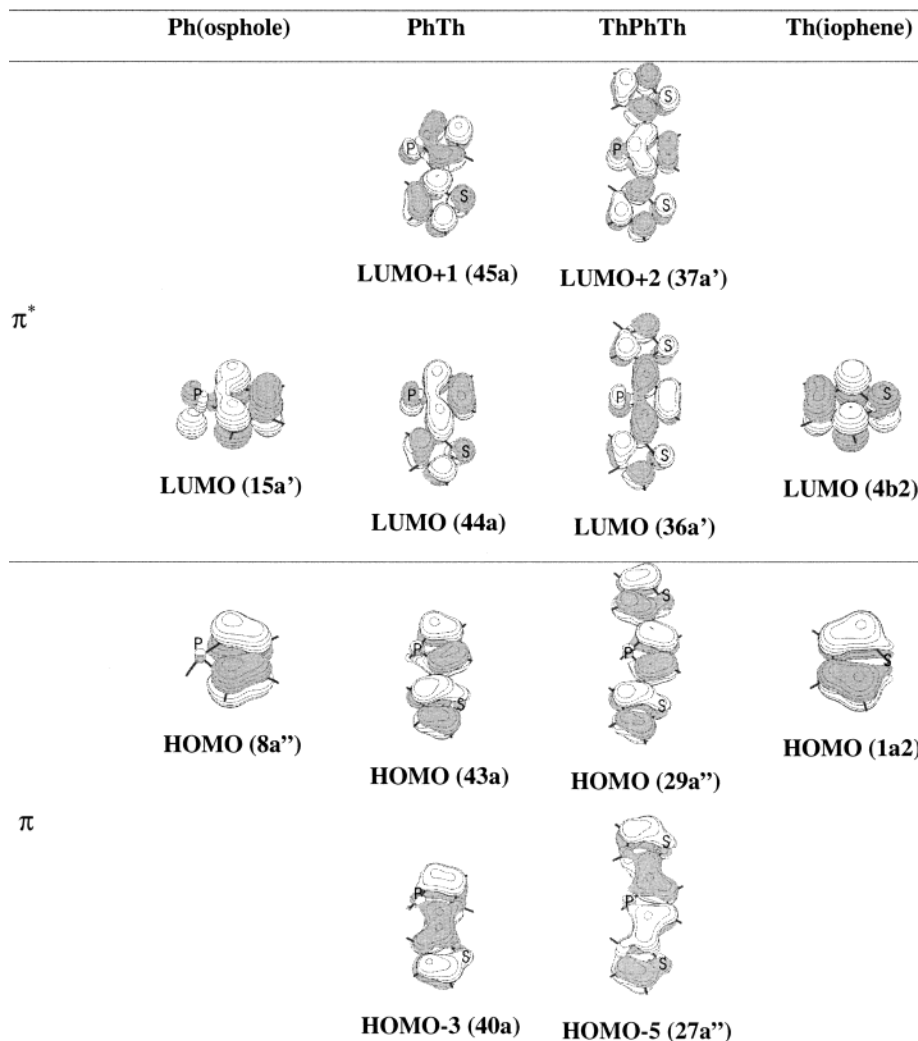


Figure 5. Shape of the π and π^* MOs involved in the orbital interaction diagrams that describe the formation of the frontier MOs of PhTh and ThPhTh.

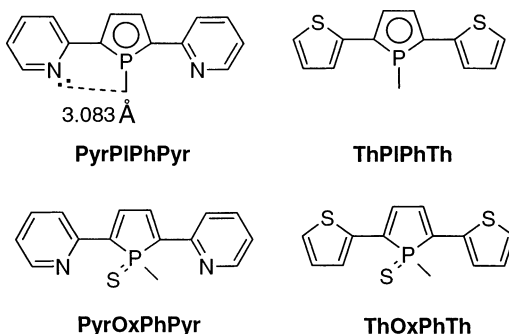


Figure 6. Structures of PyrPhPyr and ThPhTh considered with flattened and oxidized P atom, respectively.

Comparison of the structural parameters of XPIPhX with X = Pyr or Th in Table 3 with those of XPhX in Table 1 shows that the P–C and C–C bonds shorten and the C=C bonds lengthen. The JIs reach their upper limit (1.00), and the NICS values become much more negative. This confirms that flattening of the P atom results in an aromatic Ph moiety characterized by strong cyclic π -conjugation. The change of the α -values when comparing XPhX with XPIPhX points out that flattening of the P atom enforces the coplanarity between the central Ph and the pyridyl rings, whereas it increases the deviation from coplanarity between Ph and thienyl rings. The α -value for PyrPIPhPyr and ThPIPhTh amounts to 0.7 and 25.1°, respectively. The copla-

TABLE 3: Influence of Flattening or Oxidation of the P Atom on Geometric Structures of Ph and 2,5-Diheteroarylphospholes

	PIPh	PyrPIPhPyr	ThPIPhTh	OxPh	PyrOxPhPyr	ThOxPhTh
sym	C_{2v}	C_s	C_s	C_s	C_s	C_s
	Ph core					
P–C ^a	1.726	1.734	1.741	1.830	1.847	1.848
C=C	1.396	1.409	1.406	1.348	1.359	1.366
C–C	1.424	1.411	1.413	1.482	1.463	1.454
Ji	0.98	1.00	1.00	0.54	0.72	0.80
NICS ^b	–18.4	–14.4	–15.7	–1.7	–0.4	–1.0
	Interring					
α^c		0.7			18.2	6.5
$d_{C\alpha}^a$		1.460	1.451		1.463	1.443

^a Bond lengths are given in Ångstroms. ^b NICS values are given in ppm. ^c Dihedral angles are given in degrees.

narity between pyridyl and Ph is probably the result of hydrogen bond formation between P–H of Ph and the nitrogen lone pair of pyridyl as illustrated in Figure 6. The interring bond lengths ($d_{C\alpha}$) of both heteroarylphospholes are only slightly affected ($\Delta d_{C\alpha} = 0.004$ Å) when flattening the P atom. Therefore, we presume that the pronounced π -conjugation between the heteroaryl substituents and the Ph core is preserved. The presence of linear π -conjugation in XPIPhX is also reflected by the increase in Ji and NICS values when going from PIPh to XPIPhX.

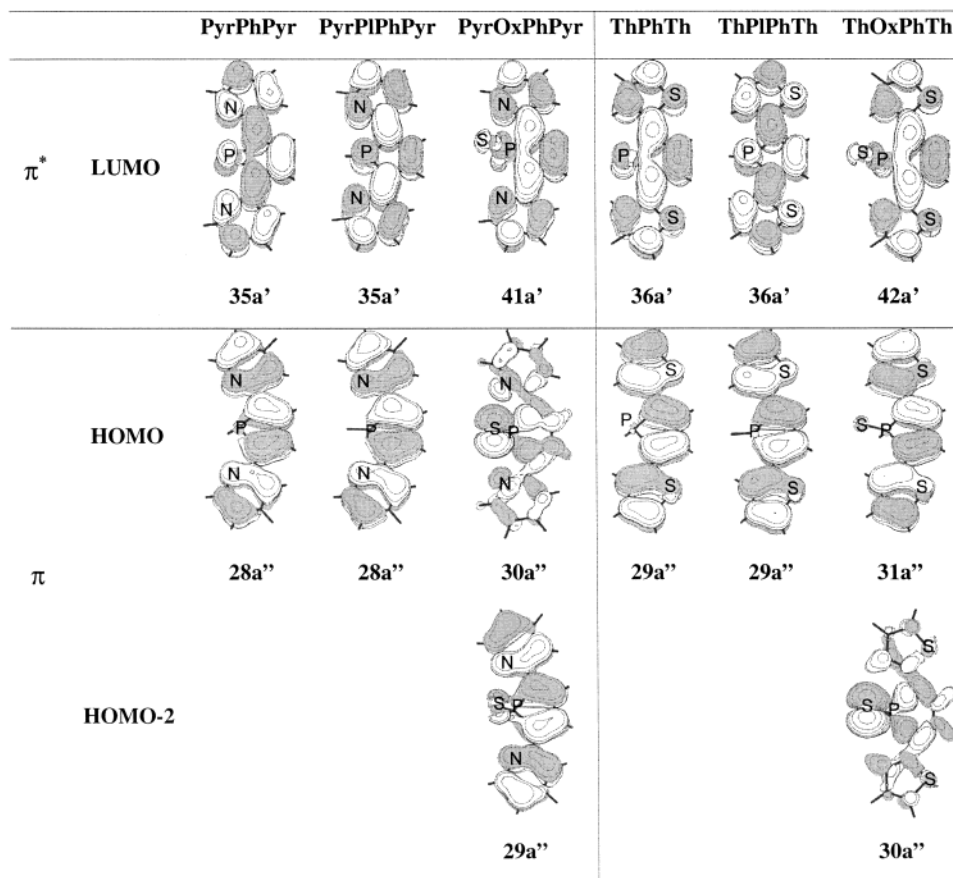


Figure 7. Shape of frontier MOs of PyrPhPyr and ThPhTh derivatives.

TABLE 4: Values of the Phosphorus IB of Ph, PyrPhPyr, and ThPhTh

	Ph	PyrPhPyr	ThPhTh
E_{\min}^a	-496.36749	-989.90321	-1599.24527
E_{ts}	-496.33831	-989.87859	-1599.20964
IB ^b	77	65	94

^a Total energies are given in Hartree. ^b Phosphorus IBs are given in kJ/mol.

Phosphorus Inversion Barrier (IB). Table 4 tabulates the values of the phosphorus IB of Ph and heteroarylphospholes. The IB of PyrPhPyr is computed to be 65 kJ/mol, which is 12 kJ/mol lower in energy than that of Ph. Stabilization of the planar transition state PyrPIPhPyr due to hydrogen bond formation between P–H of Ph and the nitrogen lone pair of pyridyl, as shown in Figure 6, appears to be a reasonable explanation for the lower IB. On the other hand, the IB of ThPhTh is calculated to be 17 kJ/mol higher in energy than that of Ph. In ThPIPhTh, there is no stabilization possible due to H-bonds and the cyclic π -conjugation in the planar Ph moiety is lowered (PIPh, NICS = -18.4; ThPIPhTh, NICS = -15.7) by a strong linear π -conjugation between thienyl and planar Ph. This destabilization of the planar Ph core due to a decrease in cyclic π -conjugation could explain the enhanced IB.

Electronic Structure. The shape of the frontier MOs of PyrPhPyr and ThPhTh derivatives is drawn in Figure 7, whereas their energies and a description of the lowest allowed singlet $\pi^* \leftarrow \pi$ transitions are presented in Table 5. Because flattening of the P atom allows a stronger interaction between the phosphorus lone pair and the *cis*-1,3-butadiene $\pi(b_1)$ orbital,^{20,21} the antibonding LUMOs of both heteroarylphospholes get destabilized by around 0.5 eV in energy. On the other hand, flattening of the P atom does not significantly influence the

HOMO energies. As a consequence, we may expect a serious increase of the reduction potential, whereas the oxidation potential should remain almost unchanged. Furthermore, we computed that the $1^1A''$ state of PyrPhPyr and ThPhThs, which involves the LUMO \leftarrow HOMO transition, is blue-shifted by 39 and 60 nm, respectively. The corresponding oscillator strengths (*f*) become stronger; therefore, we may expect more intense absorptions.

Influence of Oxidation of Phosphorus by Elemental Sulfur. Geometric Structure. A representation of 2,5-diheteroarylphospholes with an oxidized σ^4 -P atom is given in Figure 6. The influence of oxidation of phosphorus by sulfur on geometric structures is recorded in Table 3.

When comparing the structural parameters of XOxPhX with X = Pyr, Th recorded in Table 3 with those of XPhX in Table 1, we see that both the P–C and the C–C bonds lengthen but the C=C bond shortens. The JIs decrease, and the NICS values become less negative. This demonstrates that the -P(=S)R moiety switches off the cyclic π -conjugation in Ph. A larger deviation from coplanarity, as reflected by α , is found for PyrOxPhPyr as compared with PyrPhPyr (18.2 vs 5.1°), whereas a smaller deviation from coplanarity is computed for ThOxPhTh as compared with ThPhTh (6.5 vs 14.4°). Because $d_{C\alpha}$ is hardly shorter ($\Delta d_{C\alpha} \leq 0.004 \text{ \AA}$), we can conclude that oxidation of the P atom by sulfur only weakly enforces the π -conjugation between the heteroaryl substituents and the Ph. The presence of linear π -conjugation is also here reflected by the increase in JI and NICS values when going from OxPh toward XOxPhX.

Electronic Structure. Table 5 points out that oxidation of the P atom by sulfur affects both the HOMO and the LUMO of XPhX with X = Pyr or Th. As visualized in Figure 7, the HOMO of PyrPhPyr interacts in a bonding way with the sulfur

TABLE 5: Frontier Orbital Energies and a Description of the Lowest Allowed Singlet $\pi^*\leftarrow\pi$ Transitions of PyrPhPyr and ThPhTh Derivatives

		PyrPhPyr	PyrPIPhPyr	PyrOxPhPyr	ThPhTh	ThPIPhTh	ThOxPhTh
$1^1A''$	ϵ_{LUMO}^a	-2.1 (35a')	-1.6 (35a')	-2.6 (41a')	-2.1 (36a')	-1.5 (36a')	-2.6 (42a')
	ϵ_{HOMO}	-5.6 (28a'')	-5.5 (28a'')	-5.3 (30a'')	-5.2 (29a'')	-5.1 (29a'')	-5.5 (31a'')
	$\epsilon_{\text{HOMO}-2}$			-6.0 (29a'')			-6.2 (30a'')
	λ_{max}^b	383 35a' \leftarrow 28a''	344 35a' \leftarrow 28a''	648 41a' \leftarrow 30a''	429 36a' \leftarrow 29a''	369 36a' \leftarrow 29a''	468 42a' \leftarrow 31a'' 42a' \leftarrow 30a''
$2^1A''$	f^c	0.71	0.82	0.00	0.66	0.85	0.43
	λ_{max}			398 41a' \leftarrow 29a''			441 42a' \leftarrow 30a'' 42a' \leftarrow 31a''
	f			0.62			0.16

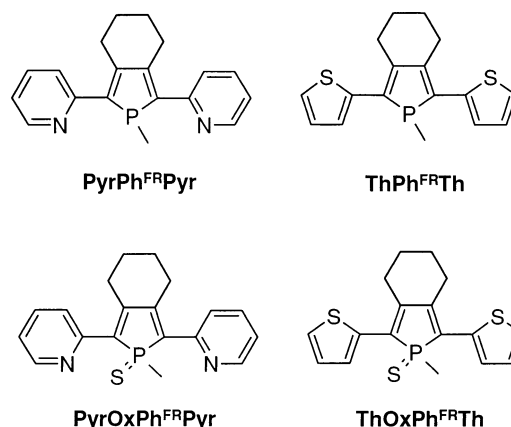
^a Frontier orbital energies are given in electronvolts. ^b Computed λ_{max} values are given in nanometers. ^c Oscillator strengths (f).

$3p_z$ orbital and results in the HOMO-2 (29a'') of PyrOxPhPyr. The HOMO (29a'') of ThPhTh undergoes a similar interaction, but at a lesser pronounced extent, and results in the HOMO (31a'') of ThOxPhTh. Table 5 shows that the HOMO-2 energy of PyrOxPhPyr is at -6.0 eV and lies 0.4 eV lower in energy than the HOMO of PyrPhPyr. The HOMO energy of ThOxPhTh is at -5.5 eV and lies thus 0.3 eV lower in energy than the HOMO of ThPhTh. When going from a σ^3 - to a σ^4 -P atom with the presence of sulfur, the LUMO of XPhX is stabilized by 0.5 eV and results in a LUMO of XOxPhX that amounts to -2.6 eV. Our computational findings agree well with the experimental electrochemical data of Réau and co-workers.⁸ Both results point out that when oxidizing the P atom by sulfur, lower reduction and higher oxidation potentials are obtained and that the oxidation potential of the thienyl compound is less reduced than that of the pyridyl counterpart.

The lowest $\pi^*\leftarrow\pi$ transition of PyrOxPhPyr with a significant oscillator strength corresponds to the LUMO \leftarrow HOMO-2 transition and the $2^1A''$ excited state. This excited state correlates with the $1^1A''$ excited state of PyrPhPyr and is red-shifted by 15 nm relative to that state. The $1^1A''$ excited state of ThOxPhTh is mainly described by the LUMO \leftarrow HOMO transition, whereas the $2^1A''$ excited state is dominated by the LUMO \leftarrow HOMO-2 transition. The oscillator strength of the $1^1A''$ state is larger than that of the $2^1A''$ state. Because the P(=S)R group more strongly stabilizes the LUMO than the HOMO, the $1^1A''$ state turns out to red shift by 39 nm when going from ThPhTh to ThOxPhTh.

Influence of a Fused, Saturated, Six-Membered Ring.
Geometric Structure. Structures of 2,5-diheteroarylphosphole derivatives that carry a saturated six-membered ring onto the Ph core are presented in Figure 8. These structures are comparable to the ones prepared and discussed by Réau and co-workers,⁶⁻⁸ except that a phenyl group on phosphorus is replaced by a hydrogen atom. Tables 6 and 7 list a selection of their geometric structure and reveal that the optimized bond lengths deviate less than 0.025 Å from the experimental (X-ray) results. On the other hand, it is difficult to compare the computed and experimental interring bond angles (α), since rotational disorder was ruled out by optimizing the structures in C_s symmetry.

Comparison of the structural parameters of XPh^{FR}X with X = Pyr or Th in Table 6 with those of XPhX in Table 1 points out that fusion of a saturated six-membered ring tends to lengthen the C-C bond by 0.02 Å. As a consequence, the conjugation over the *cis*-1,3-butadiene unit weakens, which is reflected by a smaller JI value. Because of steric interactions between the fused six-membered ring and the heteroaryl substituents, the deviation from coplanarity between central phosphole and heteroaryl rings increases from 5.1° in PyrPhPyr

**Figure 8.** Structures of 2,5-diheteroarylphosphole derivatives considered that carry a saturated six-membered ring onto the phosphole core.**TABLE 6: Geometric Structures of 2,5-Diheteroarylphosphole Derivatives that Carry a Saturated Six-Membered Ring onto the Ph Core**

	Ph ^{FR}	PyrPh ^{FR} Pyr		ThPh ^{FR} Th	
		opt	X-ray ^a	opt	X-ray ^b
sym	C_s	C_s	C_1	C_s	C_1
Ph core					
P-C ^c	1.819	1.824 1.823 ^d	1.806(6) 1.806(6)	1.835	1.817(4) 1.818(5)
C=C	1.360	1.378 1.377 ^d	1.354(8) 1.356(9)	1.376	1.336(6) 1.356(6)
C-C	1.472	1.462 1.463 ^d	1.478(9)	1.462	1.465(7)
ΣCPX^e	292.6	294.4 302.3 ^d	299.3	289.7	299.3
JI	0.68	0.82 0.81 ^d		0.81	
NICS ^f	-5.2	-4.0 -3.7 ^d		-3.7	
Interring					
α^e		27.4 30.7 ^d	25.6 7.0	29.9	16.7 12.5
dca^c		1.465 1.466 ^d	1.464(5) 1.467(5)	1.453	1.436(6) 1.457(6)

^a Ref 6. ^b Ref 7. ^c Bond lengths are given in Ångstroms. ^d Values obtained when substituting a phenyl group at the P atom. ^e Bond and dihedral angles are given in degrees. ^f NICS values are given in ppm.

to 27.4° in PyrPh^{FR}Pyr and from 14.4° in ThPhTh to 29.9° in ThPh^{FR}Th. The increase in C-C bond length and the resulting decrease in JI are also found when comparing the structural parameters of XOxPh^{FR}X in Table 7 with those of XPhX in Table 3. Also here, the deviation from coplanarity between Ph and heteroaryl rings increases from 18.2° in PyrOxPhPyr to

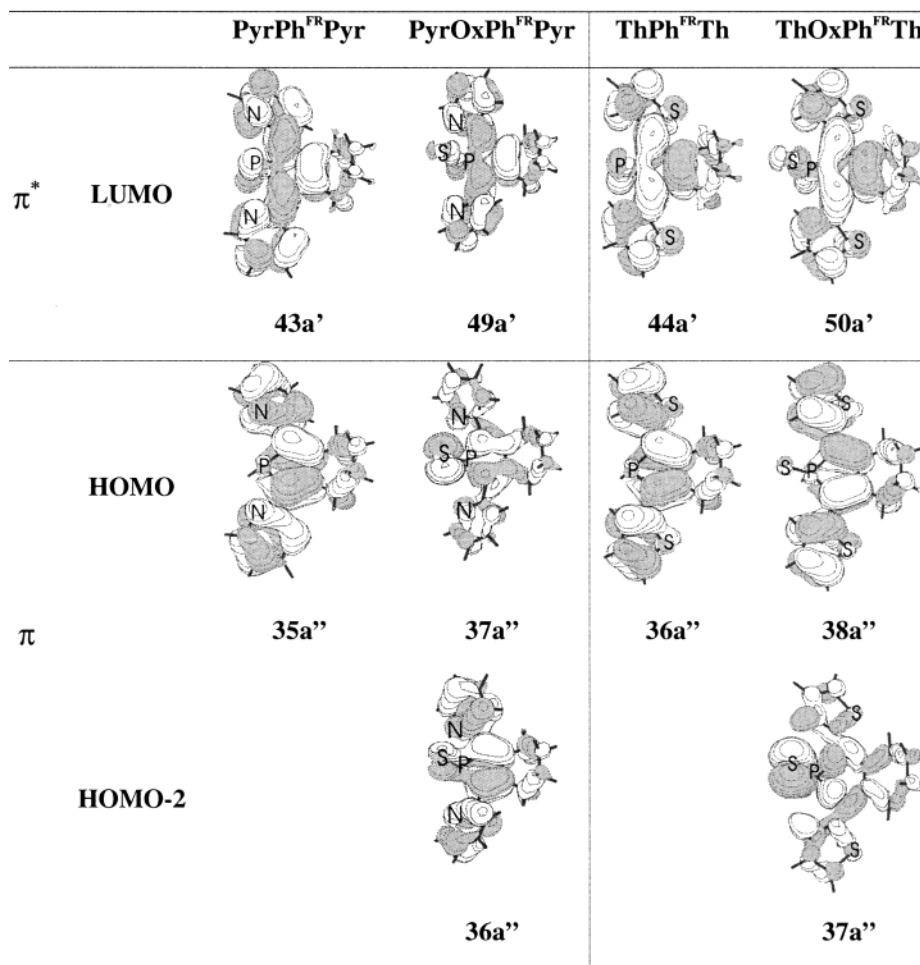


Figure 9. Shape of frontier MOs of PyrPhPyr and ThPhTh derivatives considered that carry a saturated six-membered ring onto the Ph core.

TABLE 7: Geometric Structures of Oxidized 2,5-Diheteroarylphosphole Derivatives that Carry a Saturated Six-Membered Ring

	OxPh ^{FR}	PyrOxPh ^{FR} Pyr	ThOxPh ^{FR} Th
sym	C_s	C_s	C_s
		Ph core	
P-C ^a	1.826	1.841	1.842
C=C	1.349	1.359	1.368
C-C	1.495	1.489	1.481
JI	0.45	0.57	0.68
NICS ^b	-1.7	-1.2	-0.9
		Interring	
α^c		39.6	25.0
d_{Ca^a}		1.470	1.452

^a Bond lengths are given in Ångstroms. ^b NICS values are given in ppm. ^c Dihedral angles are given in degrees.

39.6° in PyrOxPh^{FR}Pyr and from 6.5° in ThPhTh to 25.0° in ThOxPh^{FR}Th, due to steric hindrance between the fused ring and the heteroaryl substituents. The small increase of d_{Ca} indicates that the π -conjugation between Ph and heteroaryl substituents is weakened by the increased deviation from coplanarity. However, the increase in JI and NICS values when going from Ph^{FR}/OxPh^{FR} toward XPh^{FR}X/XOxPh^{FR}X proves that linear π -conjugation is still present.

Electronic Structure. The shape of the frontier MOs of XPh^{FR}X and XOxPh^{FR}X is presented in Figure 9. Their frontier orbital energies and a description of the lowest allowed singlet $\pi^* \leftarrow \pi$ transitions are given in Table 8.

TABLE 8: Frontier Orbital Energies and a Description of the Lowest Allowed Singlet $\pi^* \leftarrow \pi$ Transitions of 2,5-Diheteroarylphosphole Derivatives that Carry a Saturated Six-Membered Ring

	PyrPh ^{FR} Pyr	PyrOxPh ^{FR} Pyr	ThPh ^{FR} Th	ThOxPh ^{FR} Th
ϵ_{LUMO}^a	-1.8 (43a')	-2.1 (49a')	-1.7 (44a')	-2.3 (50a')
ϵ_{HOMO}	-5.4 (35a'')	-5.4 (37a'')	-5.1 (36a'')	-5.4 (38a'')
ϵ_{HOMO-1}				
ϵ_{HOMO-2}		-6.0 (36a'')		-6.0 (37a'')
1 ¹ A''	λ_{max}^b 372	505	403	449
	43a' \leftarrow 35a''	49a' \leftarrow 37a''	44a' \leftarrow 36a''	50a' \leftarrow 38a''
				50a' \leftarrow 37a''
2 ¹ A''	f^c 0.60	0.01	0.56	0.28
	λ_{max}^b	358	424	424
		49a' \leftarrow 36a''		50a' \leftarrow 37a''
				50a' \leftarrow 38a''
				0.19
xpt	f 395 ^d	364 ^d	412 ^e	432 ^e
	Log ϵ 4.02 ^d	3.28 ^d	3.94 ^e	3.98 ^e

^a Frontier orbital energies are given in electronvolts. ^b Computed and experimental λ_{max} values are given in nanometers. ^c Oscillator strengths (f). ^d Ref 6. ^e Ref 7.

Comparison of the frontier MOs of XPhX and XOxPhX with X = Pyr or Th in Figure 7 with those of XPh^{FR}X and XOxPh^{FR}X in Figure 9 shows that when fusing a saturated six-membered ring onto the Ph core, the order and nature of these orbitals are not really altered. Comparing their frontier orbital energies in Table 5 with respect to those tabulated in Table 8, we notice that the LUMO is more destabilized than the HOMO and HOMO-2 following ring fusion. As a consequence, the absorption wavelengths associated with the LUMO-HOMO

and/or LUMO←HOMO-2 transitions are blue-shifted. We computed that for 2,5-diheteroarylphospholes (XPhX), the blue shift upon ring fusion is more pronounced in ThPhTh ($1^1A''$: $\Delta\lambda_{\max} = 26$ nm) than in PyrPhPyr ($1^1A''$: $\Delta\lambda_{\max} = 11$ nm). On the contrary, for oxidized 2,5-diheteroarylphospholes (XOxPhX), the blue shift is more pronounced in PyrOxPhPyr ($2^1A''$: $\Delta\lambda_{\max} = 40$ nm) than in ThOxPhTh ($1^1A''$: $\Delta\lambda_{\max} = 19$ nm, $2^1A''$: $\Delta\lambda_{\max} = 17$ nm). The oscillator strengths (f) of the considered transitions are actually lowered upon fusion. The lowering is larger for XOxPhX ($\Delta f = 0.15$ – 0.19) than for XPhX ($\Delta f = 0.10$ – 0.11). Furthermore, because the LUMO is destabilized, we would predict an increase in reduction potential upon ring fusion.

Finally, Table 8 points out that the excitation energies computed with TDDFT are systematically higher and deviate less than 0.2 eV from the measured values. Furthermore, the computed and measured λ_{\max} values show a similar trend: the absorption wavelength associated with the LUMO←HOMO transition is longer in ThPh^{FR}Th than in PyPh^{FR}Py. Oxidation of the P atom causes a blue shift of this transition in PyPh^{FR}Py, but a red shift in ThPh^{FR}Th.

Conclusions

To elucidate structure–property relationships in two series of PyrPhPyr and ThPhTh derivatives containing σ^3 - or σ^4 -P atoms, we investigated in a systematic way the influence of different structural modifications on the electronic structure and emphasized the corresponding consequences for the electrochemical and optical properties. Our goal was to provide an in-depth interpretation of the UV–vis absorption spectra and electrochemical data reported earlier by Réau and co-workers.^{6–8}

We found that the more pronounced linear π -conjugation, the smaller energy gap, and the lower oxidation potential of ThPhTh derivatives can be ascribed to the stronger orbital interaction between the HOMO of Ph and the HOMO of thienyl when compared to that between the HOMO of Ph and the HOMO-1 of pyridyl in the 2,5-dipyridyl counterpart.

Furthermore, it was mentioned that the aromaticity of the Ph core can be regulated by chemical modifications at the P atom. In fact, flattening of the P atom induces strong cyclic π -conjugation, whereas it is switched off by the $-P(=S)R$ moiety. The computed interring bond lengths between the Ph and the heteroaryl substituents pointed out that those modifications at the P atom only weakly influence the linear π -conjugation. On the other hand, the electronic structure and related properties are seriously affected. For example, flattening of the P atom destabilizes the LUMO orbital, whereas the HOMO energy remains nearly the same. As a consequence, we may expect a blue shift of the wavelength associated with the LUMO←HOMO transition and an increase of the reduction potential. On the contrary, in oxidizing the P atom by sulfur, both HOMO and LUMO orbitals are stabilized, which results in lower reduction and higher oxidation potentials. However, the similarity in nature of the frontier orbitals and lowest excited states between ThPhTh and PyrPhPyr derivatives is disrupted.

Finally, we reported that fusion of a saturated six-membered ring onto the Ph core increases the deviation from coplanarity and thereby weakens the π -conjugation between Ph and heteroaryl rings. What concerns the electronic structure, we noticed that the LUMO is more destabilized than the HOMO and HOMO-2. As a result, the absorption wavelengths associated with the LUMO←HOMO and/or LUMO←HOMO-2 transitions are blue-shifted upon ring fusion. In this perspective,

we would suggest further synthetic work aiming to reduce the steric hindrance resulting from the fused rings.

Because the validation of computational methods is an important aspect within the domain of computational chemistry, we would also like to emphasize the successful use of TDDFT in evaluating quantitatively lower-lying excited states and interpreting UV–vis absorption spectra.

Acknowledgment. We thank the FWO-Vlaanderen and the Flemish government as well as the KULeuven Research Council (Concerted Research Action, GOA program) for continuing support.

References and Notes

- Freemantle, M. *Chem. Eng. News* **2001**, 79 (April 23), 49.
- Brown, A. R.; Pomp, A.; Hart, C. M.; de Leeuw, D. M. *Science* **1995**, 270, 972. Siringhaus, H.; Tessler, N.; Friend, R. H. *Science* **1998**, 280, 1741.
- (a) Tang, C. W.; Van Slyke, S. A. *Appl. Phys. Lett.* **1988**, 51, 913. (b) Burroughes, J. H.; Bradley, D. D. C.; Brown, A. R.; Marks, R. N.; Mackay, K.; Friend, R. H.; Burns, P. L.; Holmes, A. B. *Nature* **1990**, 347, 539.
- Grandstrom, M.; Petritsch, K.; Arias, A. C.; Lux, A.; Anderson, M. R.; Friend, R. H. *Nature* **1998**, 395, 257.
- Brédas, J.-L. *Adv. Mater.* **1995**, 7 (3), 263.
- Hay, C.; Le Vilain, D.; Deborde, V.; Toupet, L.; Réau, R. *Chem. Commun.* **1999**, 345.
- Hay, C.; Fischmeister, C.; Hissler, M.; Toupet, L.; Réau, R. *Angew. Chem.* **2000**, 112 (10), 1882.
- Hay, C.; Hissler, M.; Fischmeister, C.; Rault-Berthelot, J.; Toupet, L.; Nyulászi, L.; Réau, R. *Chem. Eur. J.* **2001**, 7 (19), 4222.
- (a) Mathey, F. *Chem. Rev.* **1988**, 88, 429. (b) Quin, L. D. *Comp. Heterocycl. Chem.* **1996**, 2, 757.
- Parr, R. G.; Yang, W. *Density-Functional Theory of Atoms and Molecules*; Oxford University Press: New York, 1989.
- Bauernschmitt, R.; Ahlrichs, R. *Chem. Phys. Lett.* **1996**, 256, 454.
- Ahlrichs, R.; Bär, M.; Baron, H.-P.; Bauernschmitt, R.; Böcker, S.; Ehrig, M.; Eichkorn, K.; Elliott, S.; Furche, F.; Haase, F.; Häser, M.; Horn, H.; Hättig, C.; Huber, C.; Huniar, U.; Kattannek, M.; Köhn, A.; Kölmel, C.; Kollwitz, M.; May, K.; Ochsenfeld, C.; Öhm, H.; Schäfer, A.; Schneider, U.; Treutler, O.; von Arnim, M.; Weigend, F.; Weis, P.; Weiss, H. *TURBOMOLE*, Version 5.0; University of Karlsruhe: Germany, 1998.
- Delaere, D.; Dransfeld, A.; Nguyen, M. T.; Vanquickenborne, L. G. *J. Org. Chem.* **2000**, 65, 2631.
- (a) $JI = 1 - (225/n) \sum (1 - r_j/r)^2$ and $n = 3$ and represents the number of C–C bonds. $JI = 1$ for benzene (D_{6h}) and the cyclopentadienyl ion (D_{5h}), that is, for the fully delocalized, highest symmetric systems. The empirical factor 225 provides an aromaticity scale in which $JI = 0$ for the Kekulé form of benzene (assuming 1.33 and 1.52 Å C–C lengths). (b) Julg, A.; François, P. *Theor. Chim. Acta (Berlin)* **1967**, 7, 249. (c) Schleyer, P. V. R.; Freeman, P. K.; Jiao, H.; Goldfuss, B. *Angew. Chem., Int. Ed. Engl.* **1995**, 34 (3), 337.
- Schleyer, P. V. R.; Maerker, C.; Dransfeld, A.; Jiao, H.; Hommes, N. J. R. V. E. *J. Am. Chem. Soc.* **1996**, 118, 6317.
- Frisch, M. J.; Trucks, G. W.; Schlegel, H. B.; Scuseria, G. E.; Robb, M. A.; Cheeseman, J. R.; Zakrzewski, V. G.; Montgomery, J. A., Jr.; Stratmann, R. E.; Burant, J. C.; Dapprich, S.; Millam, J. M.; Daniels, A. D.; Kudin, K. N.; Strain, M. C.; Farkas, O.; Tomasi, J.; Barone, V.; Cossi, M.; Cammi, R.; Mennucci, B.; Pomelli, C.; Adamo, C.; Clifford, S.; Ochterski, J.; Petersson, G. A.; Ayala, P. Y.; Cui, Q.; Morokuma, K.; Malick, D. K.; Rabuck, A. D.; Raghavachari, K.; Foresman, J. B.; Cioslowski, J.; Ortiz, J. V.; Stefanov, B. B.; Liu, G.; Liashenko, A.; Piskorz, P.; Komaromi, I.; Gomperts, R.; Martin, R. L.; Fox, D. J.; Keith, T.; Al-Laham, M. A.; Peng, C. Y.; Nanayakkara, A.; Gonzalez, C.; Challacombe, M.; Gill, P. M. W.; Johnson, B. G.; Chen, W.; Wong, M. W.; Andres, J. L.; Head-Gordon, M.; Replogle, E. S.; Pople, J. A. *Gaussian 98*, revision A.5; Gaussian, Inc.: Pittsburgh, PA, 1998.
- (a) Nyulászi, L. *Tetrahedron* **2000**, 56, 79. (b) Nyulászi, L. *Chem. Rev.* **2001**, 101, 1229.
- (a) Nyulászi, L.; Keglevich, Gy.; Quin, L. D. *J. Organomet. Chem.* **1996**, 61, 7808. (b) Nyulászi, L.; Soós, L.; Keglevich, Gy. *J. Organomet. Chem.* **1998**, 566, 29.
- Nyulászi, L. *J. Phys. Chem.* **1995**, 99, 586.
- Delaere, D.; Nguyen, M. T.; Vanquickenborne, L. G. *J. Organomet. Chem.* **2002**, 643, 194.
- Delaere, D.; Nguyen, M. T.; Vanquickenborne, L. G. *Phys. Chem. Chem. Phys.* **2002**, 4, 1522.